Proceedings of the 30th International Cosmic Ray Conference
Rogelio Caballero, Juan Carlos D'Olivo, Gustavo Medina-Tanco,
Lukas Nellen, Federico A. Sánchez, José F. Valdés-Galicia (eds.)
Universidad Nacional Autónoma de México,
Mexico City, Mexico, 2008
Vol. 5 (HE part 2), pages 1319–1322

30TH INTERNATIONAL COSMIC RAY CONFERENCE

Atmospheric neutrino oscillation in Super-Kamiokande

YUMIKO TAKENAGA[1] FOR SUPER-KAMIOKANDE COLLABORATION
[1]*Research Center for Cosmic Neutrinos, Institute for Cosmic Ray Research, University of Tokyo*
5-1-5 Kashiwa-no-Ha, Kashiwa-City, Chiba 277-8582 Japan
takenaga@suketto.icrr.u-tokyo.ac.jp

Abstract: The recent results on the atmospheric neutrino measurements and the oscillation analysis are presented. Using fully data for SK-I and SK-II, $\nu_\mu \leftrightarrow \nu_\tau$ two flavor oscialltion analysis is carried out with the improved method. The study for the solar oscillation effects is also performed using SK-I and SK-II data.

Introduction

The Super-Kamiokande has reported that the atmospheric neutrino data are well consistent with the pure $\nu_\mu \leftrightarrow \nu_\tau$ two flavor oscillation scheme [1, 2]. The oscillation analysis is performed using the whole data of Super-Kamiokande-I and Super-Kamiokande-II with the slightly improved analysis method to get more stringent constraint on the oscillation parameters.

The oscillation analysis including the solar neutrino oscillation parameters is also carried out using the atmospheric neutrino data. Considering the 1–2 mixing parameters which were precisely measured by combining the solar neutrino data [3, 4] and the KamLand data [5], the oscillation of the low energy (below 1 GeV) atmospheric ν_es is expected to appear at some level regardless of the existence of θ_{13} [6, 7].

The Super-Kamiokande experiment started the observation in April, 1996 and continued the data taking for five years, which period is referred to SK-I. The Super-Kamiokande-II (SK-II) started the physics measurement in January 2003 with the half of the original PMT density in the inner detector. Each inner PMT is instrumented with acrylic covers to prevent a chain reaction implosion. See [8] for more details on the detector. The analysis shown here was done using SK-I data of 1489 days exposure and SK-II data of 804 days exposure.

$\nu_\mu \leftrightarrow \nu_\tau$ two flavor oscillation analysis

Atmospheric neutrino data are categorized into fully-contained (FC), partially-contained (PC), and upward-going muon (UPμ) events and divided into 38 momentum and event type bins: the FC single-ring sub-GeV e-like (μ-like) sample, the FC single-ring multi-GeV e-like (μ-like) sample, the FC multi-ring e-like (μ-like) sample, the PC stopping (through-going) sample, and the upward stopping (through-going) muon sample. The upward through-going muons are divided into the showering and the non-showering muons. All samples are divided in 10 zenith angle bins. The definition of the event bins are same as SK-I and SK-II. To combine SK-I and SK-II, total 760 bins are used in the analysis. The number of observed events in each of 760 bins is compared with the Monte Carlo expectation by the $\nu_\mu \leftrightarrow \nu_\tau$ two flavor oscillation scheme. A χ^2 value is defined according to the Poisson probability distribution. During the fit, the expected number of events in each bin is recalculated to account for 70 systematic errors, which come from the uncertainty of the neutrino flux model, neutrino cross-section model, event selection, and the detector response. Though the systematic errors related to the event selection and the detector response are different between SK-I and SK-II, other parameters are identical for SK-I and SK-II. Among 70 systematic errors, 14 for the neutrino flux model, 12 for the interaction, 22 for the SK-I detector response and 22 for the SK-II detec-

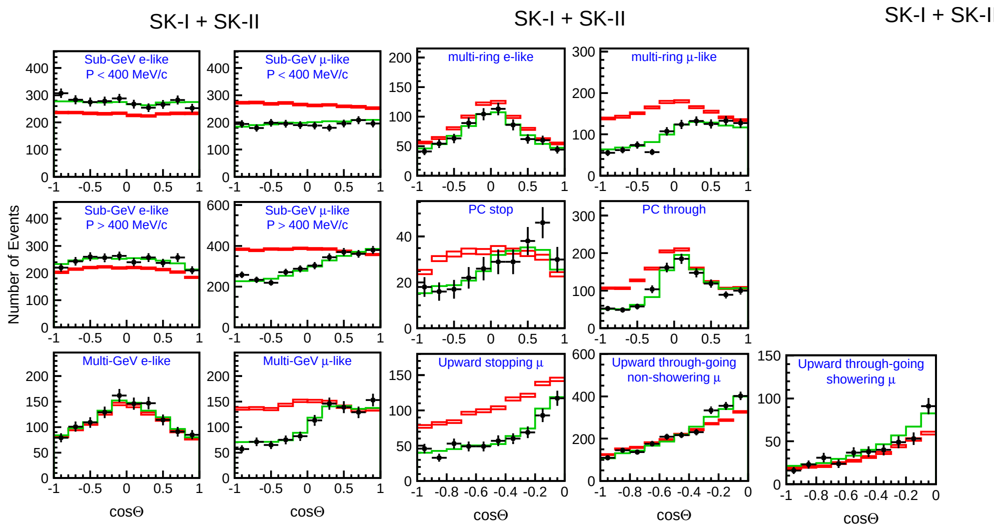

Figure 1: Zenith angle distributions of each event sample are shown for data (filled circles), Monte Carlo distributions without oscillation (box) and best-fit distributions (solid line).

tor response. Except for 6 parameters (3 for SK-I and 3 for SK-II), the parameters are common for the previous analysis described in [9]. The additional parameters are related to the solar activity, background subtraction from the upward showering muon samples, and the separation between the upward showering and non-showering muon samples. A global scan is made on a $(\sin^2 2\theta, \log\Delta m^2)$ grid minimizing χ^2 at each point with respect to 70 systematic error parameters. The minimum χ^2 value in the physical region, $\chi^2_{\rm min} = 839.7/755$ DOF, is located at $(\sin^2 2\theta = 1.00, \Delta m^2 = 2.5 \times 10^{-3}\,\mathrm{eV}^2)$. Figure 1 shows the zenith angle distribution of each data sample overlaid with non-oscillated and best fit expectations. The fitted distributions agree well with data. Figure 2 shows contours of allowed oscillation parameter regions corresponding to the 68 %, 90 %, 99 % confidence levels. The measured parameters are $\sin^2 2\theta > 0.93$ and $1.9 \times 10^{-3} < \Delta m^2 < 3.1 \times 10^{-3}$ eV^2 at 90 % confidence level.

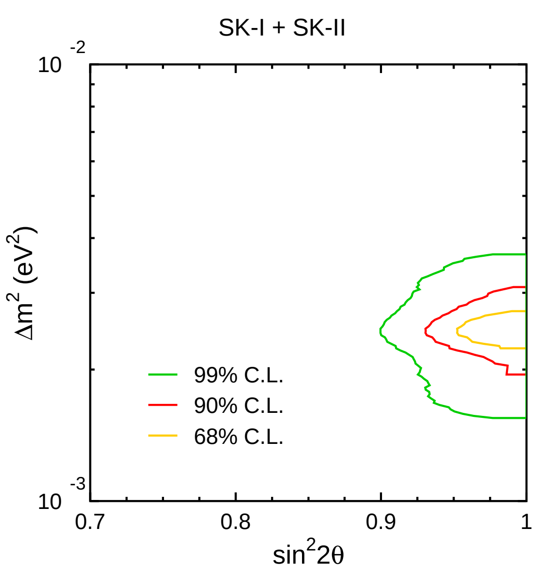

Figure 2: Allowed oscillation parameters for $\nu_\mu \leftrightarrow \nu_\tau$ oscillations by the SK-I + SK-II data

Oscillation analysis including the solar neutrino oscillation parameters

The LMA-MSW oscillation parameters measured by the solar neutrino data [3, 4] and the KamLAND reactor neutrino data [5] can lead to an observable excess of e-like events in the low energy region even if the θ_{13} is zero. We assume $\theta_{13} = 0$ here. The relative effect on the atmospheric ν_e flux is written as follows [6, 7]: $F_e^{\rm osc}/F_e^0 - 1 = P_2\,(\,r\cos^2\theta_{23} - 1\,)$, where $F_e^{\rm osc}$ and F_e^0 are the atmospheric ν_e fluxes with and without oscillations, and $r \equiv F_\mu^0/F_e^0$ is the ratio of the original atmospheric ν_μ and ν_e fluxes. P_2 is the two neutrino transition ($\nu_e \rightarrow \nu_x$) probability in matter driven by the 1–2 parameters. The factor in brackets in the equation is called the "screening" factor. In sub-GeV region $r \sim 2$, therefore the screening factor is very small for the maximal 2–3 mixing. According to the screening factor, the appearance of the sub-dominant oscillation effect depends largely on the deviation of $\sin^2 2\theta_{23}$ from the maximal. If θ_{23} is in the first octant ($\theta_{23} < 45°$), the screening factor is positive and an excess of the sub-GeV e-like sample is expected. If θ_{23} is in the second octant ($\theta_{23} > 45°$), the screening factor is negative and the sub-GeV e-like sample is expected to be reduced. Thus, the oscillation analysis including the sub-dominant 1–2 oscillation effects has the possibility to determine the octant of θ_{23} for the non-maximal $\sin^2 2\theta_{23}$. The deviation of $\sin^2 2\theta_{23}$ from unity affects the other observables, especially the zenith angle dependence of μ-like events. Therefore we need a combined oscillation analysis of all the samples with systematic errors properly estimated.

Since $\theta_{13} = 0$ is assumed in this analysis, χ^2 is calculated in the four dimensional oscillation parameter space of Δm^2_{12}, Δm^2_{23}, $\sin^2\theta_{12}$ and $\sin^2\theta_{23}$. For the solar neutrino parameters, we examine two scenarios. In the scenario with the solar neutrino parameters turned on, the solar neutrino parameters are chosen around the allowed region obtained by a combined analysis of the solar neutrino data and KamLAND data. To take into account the constraint on the solar neutrino parameters, the χ^2 value by the combined analysis of the solar neutrino and KamLAND data is added to χ^2 from the atmospheric neutrino data for each (Δm^2_{12} , $\sin^2\theta_{12}$) point. The other scenario is ordinary "one mass scale dominance" approximation with $\Delta m^2_{12} = 0$, that is, pure $\nu_\mu \leftrightarrow \nu_\tau$ two flavor oscillation scenario. The data set and its binning, the definition of χ^2 and its minimization at each oscillation parameter point, and the systematic errors are the same as those of the two flavor zenith angle analysis described in this paper. Figure 3 shows the $\sin^2\theta_{23}$ dependence of the $\chi^2 - \chi^2_{\rm min}$ function marginalized with respect to Δm^2_{12}, Δm^2_{23} and $\sin^2\theta_{12}$, for two scenarios with and without the solar neutrino parameters. We did not find any evidence for θ_{23} deviationg from the maximal value $(45°)$

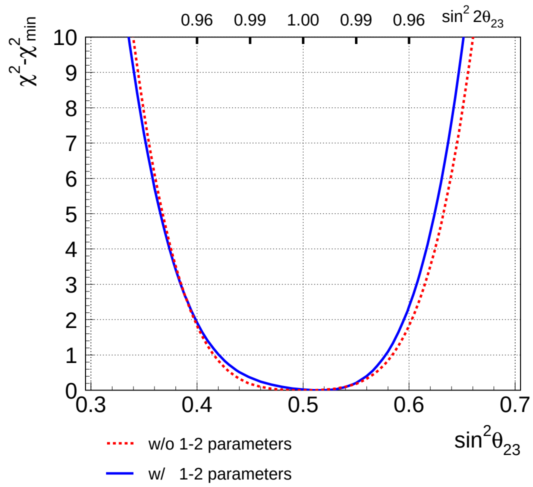

Figure 3: The $\chi^2 - \chi^2_{\rm min}$ distribution as a function of $\sin^2\theta_{23}$ for oscillations without the 1–2 parameters (red dashed line) and with the 1–2 parameters (blue solid line) by the SK-I + SK-II atmospheric neutrino data. $\theta_{13} = 0$ is assumed. For each $\sin^2\theta_{23}$ point, the other oscillation parameters are chosen to minimize χ^2.

Conclusions

In summary, a $\nu_\mu \leftrightarrow \nu_\tau$ two flavor oscillation analysis was carried out with SK-I and SK-II combined dataset. The region of $\sin^2 2\theta > 0.93$ and $1.9 \times 10^{-3} < \Delta m^2 < 3.1 \times 10^{-3}$ eV^2 is allowed at 90 % confidence level. An oscillation analysis including the solar neutrino parameters was performed and no significant change on the result of the analysis without the solar parameters was observed.

Acknowledgements

We gratefully acknowledge the cooperation of the Kamioka Mining and Smelting Company. The Super-Kamikande experiment has been built and operated from funding by the Japanese Ministry of Education, Culture, Sports, Science and Technology, the United States Department of Energy, and the U.S. National Science Foundation, and the National Natural Science Foundation of China. The author was supported by the COE21 program "Quantum Extreme Systems and their Symmetries".

References

[1] Y. Fukuda, et al., Phys. Rev. Lett. 81 (1998) 1562–1567.
[2] Y. Ashie, et al., Phys. Rev. D71 (2005) 112005.
[3] S. N. Ahmed, et al., Phys. Rev. Lett. 92 (2004) 181301.
[4] J. Hosaka, et al., Phys. Rev. D73 (2006) 112001.
[5] T. Araki, et al., Phys. Rev. Lett. 94 (2005) 081801.
[6] O. L. G. Peres, A. Y. Smirnov, Phys. Lett. B456 (1999) 204–213.
[7] O. L. G. Peres, A. Y. Smirnov, Nucl. Phys. B680 (2004) 479–509.
[8] Y. Fukuda, et al., Nucl. Instrum. Meth. A501 (2003) 418–462.
[9] J. Hosaka, et al., Phys. Rev. D74 (2006) 032002.